



ACADÉMIE
DES SCIENCES
INSTITUT DE FRANCE

Comptes Rendus

Mathématique


Maxim Arnold and Carlos E. Arreche

Symmedians as Hyperbolic Barycenters

Volume 362 (2024), p. 1743-1762

Online since: 25 November 2024

<https://doi.org/10.5802/crmath.677>

 This article is licensed under the
CREATIVE COMMONS ATTRIBUTION 4.0 INTERNATIONAL LICENSE.
<http://creativecommons.org/licenses/by/4.0/>



*The Comptes Rendus. Mathématique are a member of the
Mersenne Center for open scientific publishing*
www.centre-mersenne.org — e-ISSN : 1778-3569



Research article / *Article de recherche*
Geometry and Topology / *Géométrie et Topologie*

Symmedians as Hyperbolic Barycenters

Symédianes comme barycentres hyperboliques

Maxim Arnold^a and Carlos E. Arreche^{*,a}

^a Department of Mathematical Sciences, The University of Texas at Dallas,
Richardson, TX 75080, USA

E-mails: Maxim.Arnold@utdallas.edu, Arreche@utdallas.edu

Abstract. The symmedian point of a triangle enjoys several geometric and optimality properties, which also serve to define it. We develop a new dynamical coordinatization of the symmedian, which naturally generalizes to other ideal hyperbolic polygons beyond triangles. We prove that in general this point still satisfies analogous geometric and optimality properties to those of the symmedian, making it into a hyperbolic barycenter. We initiate a study of moduli spaces of ideal polygons with fixed hyperbolic barycenter, and of some additional optimality properties of this point for harmonic (and sufficiently regular) ideal polygons.

Résumé. Le point symédiane d'un triangle possède plusieurs propriétés géométriques d'optimalité, qui peuvent servir à la définir. Nous développons une nouvelle définition dynamique du point symédiane, qui se généralise naturellement à d'autres polygones idéaux hyperboliques, au-delà des triangles. Nous prouvons que, de manière générale, ce point satisfait toujours des propriétés géométriques d'optimalité analogues à celles du point symédiane, qui en font un barycentre hyperbolique. Nous entamons une étude des espaces de modules des polygones idéaux dont le barycentre hyperbolique est fixe, ainsi que de certaines propriétés d'optimalité supplémentaires pour les polygones idéaux harmoniques (et suffisamment réguliers).

Keywords. symmedian point, Hyperbolic barycenter, harmonic polygon, ideal hyperbolic polygon.

Mots-clés. Barycentre hyperbolique, polygone harmonique, polygone hyperbolique idéal.

2020 Mathematics Subject Classification. 51M15, 52C30, 51A45, 53A70.

Manuscript received 19 November 2023, revised 23 May 2024 and 12 August 2024, accepted 13 August 2024.

1. Introduction

The *symmedian point* of a triangle (also called its *Lemoine point* or its *Grebe point*) has been aptly called “one of the crown jewels of modern geometry” in [12, Section 7.1]. Let us recall one way to construct it (cf. [12, Section 7.4(iii)]). Let \mathbf{O} denote the circumcircle of $\Delta(ABC)$. Denote by A^* the intersection of the tangents to \mathbf{O} at the vertices B and C , and define B^* and C^* analogously. Then the lines AA^* , BB^* and CC^* are concurrent at the *symmedian point* S of the triangle ABC .

Among very many other properties enjoyed by the symmedian point S , there is the following optimization property, which is included as Exercise 7.3 in [12], and has been known (and reproved multiple times) since at least 1804 (cf. [14, p. 94]).

*Corresponding author

Theorem 1. *The symmedian point S of a triangle minimizes the sum of the squares of the distances from S to the sides of the triangle.*

The construction of the symmedian point of a triangle described in Figure 1 is particularly suggestive to the hyperbolic geometer. In the *Beltrami–Cayley–Klein model*, the hyperbolic plane \mathbb{H} is identified with the interior of the unit disc in \mathbb{R}^2 . Geodesics are represented by straight lines, but the hyperbolic angles between geodesics do not in general agree with the corresponding Euclidean angles. The unit circle boundary of this disc, called the *absolute*, represents “ideal points” at infinite hyperbolic distance from any given point in \mathbb{H} . If we interpret the circle \mathbf{O} in Figure 1 as the absolute in the Beltrami–Cayley–Klein model, we can interpret the Euclidean triangle $\Delta(ABC)$ as an ideal hyperbolic triangle with “the same” vertices — we emphasize that the idea of “hyperbolizing” Euclidean geometric objects is not new, see e.g. [2, 8]. The point A^* is called the *polar* to the line BC with respect to \mathbf{O} , and any geodesic through A^* intersects BC orthogonally in \mathbb{H} . Therefore, the symmedian point of $\Delta(ABC)$ is the point of intersection of its hyperbolic altitudes, i.e., its hyperbolic orthocenter.

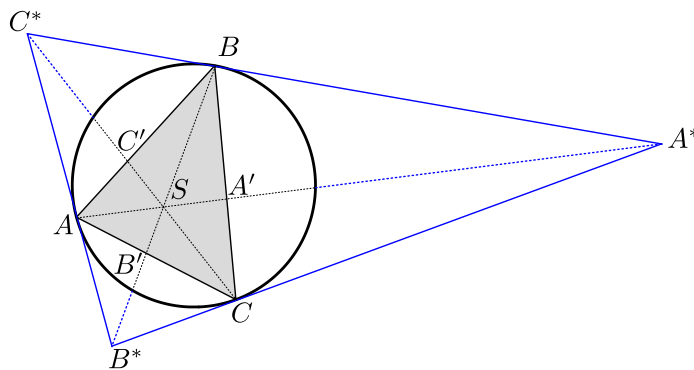


Figure 1. Construction of the symmedian point S of the triangle $\Delta(ABC)$.

This simple observation readily provides another minimality property of the symmedian point S , complementary to Theorem 1 but this time hyperbolic, as follows. For any triangle $\Delta(ABC)$ and a given point X , consider the *Cevian triangle* $\Delta(A'B'C')$, where A' is the intersection of the geodesic AX with the side BC , and the points B' and C' are defined similarly.

Theorem 2. *The symmedian point of $\Delta(ABC)$ minimizes the hyperbolic perimeter of its Cevian triangle.*

Proof. This follows from the classic reflection argument about Fargano’s orbit: under sequential hyperbolic reflections of the triangle ABC in its sides, the sides of the triangle $A'B'C'$ form a geodesic interval (see Figure 2). \square

Our main goal is to introduce a generalization of the symmedian point S of a triangle to inscribed polygons (or what is “the same”, ideal hyperbolic polygons), which we call the *hyperbolic barycenter*, and initiate a study of its properties. This point is uniquely defined in three different ways: by explicit coordinates (3.3), by an optimality property (see Theorem 5), and by a collection of geometric constructions (see Section 4), all directly analogous to those identifying the symmedian point of a triangle. We have the sense of having opened some long-forgotten Pandora’s box, and we have now more questions than answers. We have striven to make this work as accessible as possible so that other researchers (including students!) may better address the questions

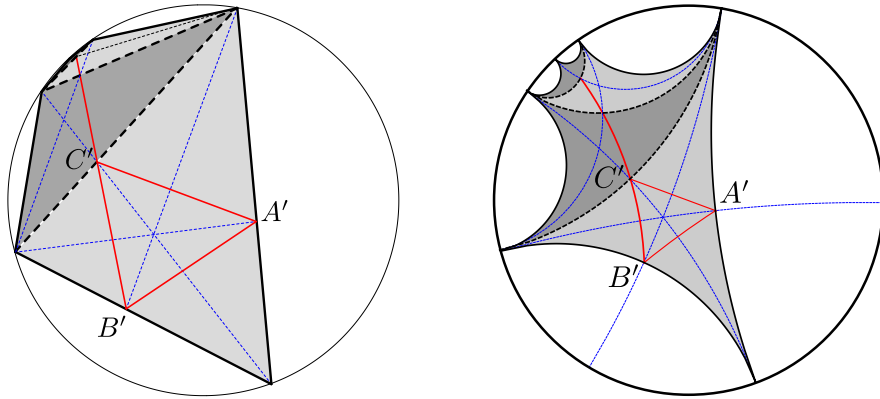


Figure 2. Another minimality property of the Symmedian point, from both the Beltrami–Cayley–Klein (left) and the Poincaré (right) points of view.

that we leave unanswered. We hope that the more sophisticated reader will not begrudge us our choice to keep the exposition, constructions, and proofs as elementary as we knew how.

Let us briefly describe the contents of this work in some more detail. In Section 2, we recall some basic facts from hyperbolic geometry, and fix some conventions that will help us navigate as needed between the *hyperboloid model*, which leads to very natural proofs of our main theoretical results, and the Beltrami–Cayley–Klein model mentioned above, which begs the interplay between Euclidean and hyperbolic geometry, and is also more amenable to pictures. In Section 3 we introduce a dynamical coordinatization of this S , in terms of certain Hamiltonians introduced in [4] for the study of cross-ratio dynamics on ideal polygons, and use it to prove another minimality property in Theorem 5, which makes S into a hyperbolic barycenter. We then introduce the hyperbolic barycenters of general ideal hyperbolic polygons, and prove several interesting and useful properties that, in particular, allow for their several concurrent geometric (straightedge and compass) constructions. In Section 4 we illustrate some of these geometric constructions for the first few ideal hyperbolic n -gons beyond triangles, with $n = 4, 6, 10, 5$, and begin to see how the hyperbolic barycenter serves as the epicenter of a dizzying cascade of concurrences, which triangles are too small to let us see. In Section 5 we initiate the study of the moduli spaces of ideal hyperbolic n -gons with a fixed common hyperbolic barycenter, and describe it explicitly for the smallest values of $n = 3, 4$ in terms of Poncelet conics. In Section 6 we show that the classical Theorem 1 is the first instance of a more general Theorem 33 that holds uniformly for all *harmonic* ideal hyperbolic polygons, and we prove a partial converse in Theorem 35 for ideal hyperbolic quadrilaterals. We conclude in Section 7 with some remaining questions concerning hyperbolic barycenters, which we submit deserve further exploration.

2. Elements of hyperbolic geometry

There are many models of the same hyperbolic plane \mathbb{H} besides the Beltrami–Cayley–Klein model discussed above. Although the latter conveniently superimposes hyperbolic geometry and (inscribed) Euclidean geometry, and thus served as the initial motivation for this work, it is not the most advantageous model for some of our purposes.

Let us now briefly describe the *hyperboloid model* of the hyperbolic plane, and fix some notation and conventions along the way – we refer to [15] and the references therein for a more

systematic treatment. We work within the ambient *Minkowski space* $\mathbb{R}^{2,1}$, whose set of points $\mathbf{x} = (x_0, x_1, x_2)$ is endowed with the *Minkowski bilinear form*

$$\langle \mathbf{x}, \mathbf{y} \rangle := -x_0y_0 + x_1y_1 + x_2y_2. \tag{2.1}$$

and its associated *Minkowski (squared) norm* $\|\mathbf{x}\| := \langle \mathbf{x}, \mathbf{x} \rangle = -x_0^2 + x_1^2 + x_2^2$. The level sets of the Minkowski norm foliate $\mathbb{R}^{2,1}$ into three kinds of (possibly degenerate; possibly one-sheeted or two-sheeted) hyperboloids, according to whether the norm is zero, positive, or negative. We shall identify the hyperbolic plane with the upper sheet of the two-sheeted hyperboloid of points with Minkowski norm -1 :

$$\mathbb{H} := \{ \mathbf{x} = (x_0, x_1, x_2) \in \mathbb{R}^{2,1} \mid \|\mathbf{x}\| = -1 \text{ and } x_0 > 0 \}. \tag{2.2}$$

We shall also refer to the *light cone* \mathbb{L} , consisting of points with vanishing Minkowski norm, and to the *de Sitter space* \mathbb{S} , consisting of points with Minkowski norm 1:

$$\mathbb{L} := \{ \mathbf{x} \in \mathbb{R}^{2,1} \mid \|\mathbf{x}\| = 0 \} \quad \text{and} \quad \mathbb{S} := \{ \mathbf{x} \in \mathbb{R}^{2,1} \mid \|\mathbf{x}\| = 1 \}. \tag{2.3}$$

For any set V of vectors in Minkowski space $\mathbb{R}^{2,1}$ we write $\mathbb{R}V$ for their \mathbb{R} -linear span, except in the case of a singleton where we simply write $\mathbb{R}\mathbf{x}$ or $[x_0 : x_1 : x_2]$ instead of $\mathbb{R}\{\mathbf{x}\}$.

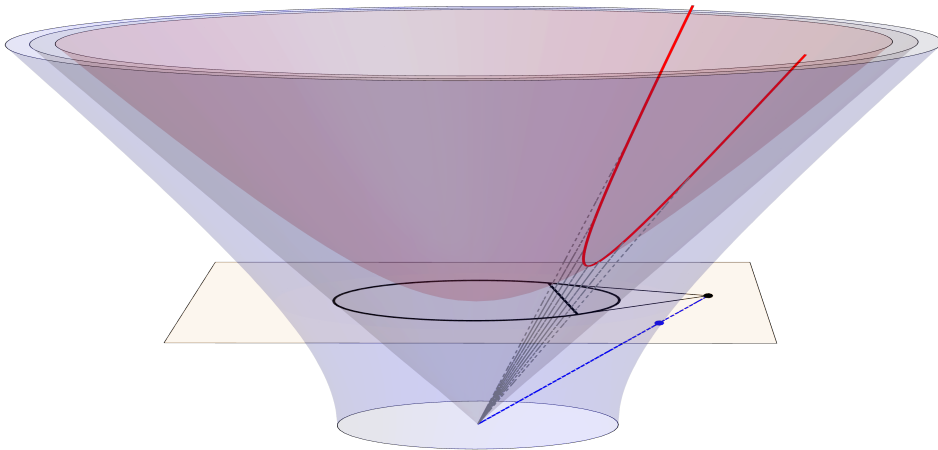


Figure 3. The Beltrami–Cayley–Klein model and the hyperboloid model embedded in $\mathbb{R}^{2,1}$.

In the hyperboloid model, the role of the absolute \mathbf{O} is played by the lines of $\mathbb{R}^{2,1}$ contained in the light cone \mathbb{L} . This absolute is identified stereographically with $\mathbb{R} \cup \{\infty\} \simeq \mathbb{R}\mathbb{P}^1$ (see e.g. [7]), by associating with ∞ the line $[1, -1, 0] \subset \mathbb{L}$, and with $\infty \neq p \in \mathbb{R}\mathbb{P}^1$ the line in \mathbb{L} given by

$$\ell(p) := [1 + p^2 : 1 - p^2 : 2p]. \tag{2.4}$$

Writing $p = \tan(\varphi/2)$ yields the usual parametrization $[1 : \cos \varphi : \sin \varphi]$ of the pencil of lines in \mathbb{L} .

The geodesic lines ξ in \mathbb{H} are precisely the intersections of hyperplanes through the origin in $\mathbb{R}^{2,1}$ having non-empty intersection with \mathbb{H} , or equivalently, such that their perpendicular complements $(\mathbb{R}\xi)^\perp$ (with respect to the Minkowski inner product) have non-empty intersection with de Sitter space \mathbb{S} . Note that in this case we always have $(\mathbb{R}\xi)^\perp \cap \mathbb{S} = \{\pm \xi^*\}$, a pair of antipodal points in \mathbb{S} called the *polars* of ξ , and choosing one *principal polar* ξ^* over the other is tantamount to endowing the hyperplane $(\mathbb{R}\xi^*)^\perp = \mathbb{R}\xi \subset \mathbb{R}^{2,1}$ with an orientation. An equivalent way to specify the non-oriented geodesic line ξ is by the set of lines $\mathbb{R}\xi \cap \mathbb{L} = \{\ell(p_1), \ell(p_2)\}$, with

notation as in (2.4). We shall distinguish between the two possible choices of orientation by writing $\xi(p_1, p_2)$ for the oriented geodesic line whose principal polar is

$$\xi^*(p_1, p_2) := \left(\frac{1 + p_1 p_2}{p_1 - p_2}, \frac{1 - p_1 p_2}{p_1 - p_2}, \frac{p_1 + p_2}{p_1 - p_2} \right) \in \mathbb{S}; \tag{2.5}$$

so that $\xi(p_1, p_2) = \{ \mathbf{x} \in \mathbb{H} \mid \langle \mathbf{x}, \xi^*(p_1, p_2) \rangle = 0 \}$.

Thus, although $\xi(p_1, p_2)$ and $\xi(p_2, p_1)$ coincide as subsets of \mathbb{H} , their principal polars form an antipodal pair in \mathbb{S} , i.e., $\xi^*(p_1, p_2) = -\xi^*(p_2, p_1)$.

The hyperbolic distance between two points $\mathbf{x}, \mathbf{y} \in \mathbb{H}$ is defined by

$$d(\mathbf{x}, \mathbf{y}) := \cosh^{-1}(-\langle \mathbf{x}, \mathbf{y} \rangle), \tag{2.6}$$

where $\cosh(t) := \frac{1}{2}(e^t + e^{-t})$ denotes the hyperbolic cosine. The hyperbolic distance between a point $\mathbf{x} \in \mathbb{H}$ and a geodesic line $\xi \subset \mathbb{H}$, defined as $\inf\{d(\mathbf{x}, \mathbf{y}) \mid \mathbf{y} \in \xi\}$, can be seen to coincide with

$$d(\mathbf{x}, \xi) = \cosh^{-1} \sqrt{1 + \langle \mathbf{x}, \xi^* \rangle^2}, \tag{2.7}$$

for $\xi^* \in \mathbb{S}$ any polar of ξ . Indeed, the closest point in ξ to \mathbf{x} is $\mathbb{R}\{\mathbf{x}, \xi^*\} \cap \xi = \{\mathbf{y}\}$, which is given by

$$\mathbf{y} = \left(1 + \langle \mathbf{x}, \xi^* \rangle^2 \right)^{-\frac{1}{2}} \cdot (\mathbf{x} - \langle \mathbf{x}, \xi^* \rangle \xi^*),$$

whence (2.7) follows directly from (2.6).

Remark 3. The Beltrami–Cayley–Klein model can now be considered as embedded in Minkowski space $\mathbb{R}^{2,1}$ within the $x_0 = 1$ plane, and is connected to the hyperboloid model by drawing lines through the origin in $\mathbb{R}^{2,1}$. More precisely, for $\mathbf{x} = (x_0, x_1, x_2) \in \mathbb{H}$ as in (2.2) we can consider

$$X = (x_1/x_0, x_2/x_0) =: \check{\mathbf{x}}.$$

This is called the *gnomonic projection* of the hyperboloid \mathbb{H} . Conversely, given a point $X = (x_1, x_2)$ in the Beltrami–Cayley–Klein model of the hyperbolic plane we can consider the corresponding point on the hyperboloid model

$$\mathbf{x} = (1 - x_1^2 - x_2^2)^{-\frac{1}{2}} \cdot (1, x_1, x_2) =: \widehat{X}.$$

Similar formulas relate antipodal pairs of points in de Sitter space \mathbb{S} with the points in the exterior of the unit circle (together with a circle at infinity) which correspond to polars of geodesics in the Beltrami–Cayley–Klein model. Finally, points on the absolute in the Beltrami–Cayley–Klein model correspond to lines in the light cone \mathbb{L} .

3. Coordinates and hyperbolic properties of the symmedian

Suppose $p_1, \dots, p_n \in \mathbb{R}^{\mathbb{P}^1}$ are sequentially distinct, meaning that $p_t \neq p_{t+1}$, where we understand indices modulo n , that is, with $p_{n+1} := p_1$. We denote by $\mathbf{P} = (p_1, \dots, p_n)$ the *ideal hyperbolic polygon* \mathbf{P} whose ideal vertices lie on $\ell(p_t) \in \mathbb{L}$ as in (2.4) and whose sides are given by (2.5). We insist that this notation and description, like hyperbolic geometry, does not actually privilege any of the models of \mathbb{H} embedded in Minkowski space $\mathbb{R}^{2,1}$. Whenever we wish to restrict ourselves to working within the Beltrami–Cayley–Klein model (resp., in the hyperboloid model), we shall emphasize this by writing $\check{\mathbf{P}}$ (resp., $\widehat{\mathbf{P}}$), to make this clear and unambiguous. Whenever we need to assume that \mathbf{P} is *convex*, we shall always state this explicitly. Note that a non-convex ideal hyperbolic polygon is necessarily self-intersecting.

An ideal polygon $\mathbf{P} = (p_1, \dots, p_n)$ being given, we shall write from now on, for the sake of brevity,

$$I_t = \frac{1}{p_t - p_{t+1}}, \quad J_t = \frac{1}{2} \frac{p_t + p_{t+1}}{p_t - p_{t+1}}, \quad K_t = \frac{p_t p_{t+1}}{p_t - p_{t+1}}. \tag{3.1}$$

Note that here the arithmetic operations from \mathbb{R} are extended to $\mathbb{R} \cup \{\infty\} \simeq \mathbb{R}P^1$ in the usual way, as is already implicit in (2.5). Thus the coordinates of the principal polars (2.5) are given by $\xi^*(p_t, p_{t+1}) = (I_t + K_t, I_t - K_t, 2J_t)$. The following quantities were introduced in [4, Section 6.2], where they were shown to be Hamiltonians for the infinitesimal diagonal action of the Möbius group:

$$I_{\mathbf{P}} = \sum_{t=1}^n I_t, \quad J_{\mathbf{P}} = \sum_{t=1}^n J_t, \quad K_{\mathbf{P}} = \sum_{t=1}^n K_t. \tag{3.2}$$

Theorem 4. *The symmedian point $\check{S}_{\mathbf{P}}$ of $\check{\mathbf{P}} = (p_1, p_2, p_3)$ is*

$$\check{S}_{\mathbf{P}} = \left(\frac{I_{\mathbf{P}} - K_{\mathbf{P}}}{I_{\mathbf{P}} + K_{\mathbf{P}}}, \frac{2J_{\mathbf{P}}}{I_{\mathbf{P}} + K_{\mathbf{P}}} \right). \tag{3.3}$$

Proof. It is an elementary computation that $\check{S}_{\mathbf{P}}$ is the intersection of the three planes through $\ell(p_t)$ and $\xi_{p_{t-1}, p_{t+1}}^*$ for $t = 1, 2, 3$ with the Beltrami–Cayley–Klein hyperbolic plane at $x_0 = 1$. \square

We can now show another minimality property of the symmedian point, which makes it into a kind of “hyperbolic barycenter”. We find it convenient to state this next result in a format that does not privilege either of our particular models of \mathbb{H} in $\mathbb{R}^{2,1}$.

Theorem 5. *If \mathbf{P} is convex, then the point $S_{\mathbf{P}} := \mathbb{H} \cap [I_{\mathbf{P}} + K_{\mathbf{P}} : I_{\mathbf{P}} - K_{\mathbf{P}} : 2J_{\mathbf{P}}]$ as in (3.3) minimizes the sum of the hyperbolic sines of the hyperbolic distances to the sides of \mathbf{P} .*

Proof. The convexity of \mathbf{P} ensures that the sought minimizer lies in the (closed) interior of \mathbf{P} , for the reflection of an exterior point with respect to the side to which it is closest results in a new point that is strictly closer to each of the remaining sides. The identity $\cosh^{-1}(t) = \sinh^{-1}(\sqrt{t^2 - 1})$ together with (2.7) yield, for the hyperbolic distance $d(\mathbf{x}, \xi_t)$ from a point $\mathbf{x} = (x_0, x_1, x_2) \in \mathbb{H}$ to the side $\xi_t := \xi(p_t, p_{t+1})$, with principal polar $\xi_t^* := \xi^*(p_t, p_{t+1})$ as in (2.5), that

$$q_t(\mathbf{x}) := \sinh(d(\mathbf{x}, \xi_t)) = |\langle \mathbf{x}, \xi_t^* \rangle|. \tag{3.4}$$

We then see that $\sum_t q_t(\mathbf{x}) = |\langle \mathbf{x}, \sum_t \xi_t^* \rangle|$ for any \mathbf{x} in the interior of \mathbf{P} , and therefore the minimum is achieved at $\mathbb{H} \cap \mathbb{R} \sum_t \xi_t^*$. We see from (2.5) and (3.2) that $\sum_t \xi_t^* = (I_{\mathbf{P}} + K_{\mathbf{P}}, I_{\mathbf{P}} - K_{\mathbf{P}}, 2J_{\mathbf{P}})$. The non-obvious and necessary fact that $[I_{\mathbf{P}} + K_{\mathbf{P}}, I_{\mathbf{P}} - K_{\mathbf{P}}, 2J_{\mathbf{P}}]$ indeed intersects \mathbb{H} in the interior of \mathbf{P} follows from Theorem 4 in the case of triangles, and is proved for general convex \mathbf{P} in Corollary 15 below. \square

Remark 6. It is easy to see that $I_{\mathbf{P}} + K_{\mathbf{P}} \neq 0$, not just generically, but always when \mathbf{P} is convex. Parameterizing $p_t = \tan(\varphi_t/2)$, each $I_t + K_t = \frac{1+p_t p_{t+1}}{p_t - p_{t+1}} = \cot\left(\frac{\varphi_t - \varphi_{t+1}}{2}\right)$. At most one $I_t + K_t$ has different sign from the others (only in case $|\varphi_t - \varphi_{t+1}| \geq \pi$). Even in this exceptional case, since $|\varphi_{t'} - \varphi_{t'+1}| < 2\pi - |\varphi_t - \varphi_{t+1}|$ for any other $t' \neq t$, we obtain immediately that $|I_{t'} + K_{t'}| > |I_t + K_t|$.

The convexity of \mathbf{P} is what ensures that the signs of the $\langle \mathbf{x}, \xi_t^* \rangle$ in (3.4) are all the same, since in this case the interior of \mathbf{P} is precisely the intersection of \mathbb{H} with all the half-spaces defined by $\langle \bullet, \xi_t^* \rangle \geq 0$ (resp., ≤ 0) in case the ideal vertices of \mathbf{P} are oriented counterclockwise (resp., clockwise). We discuss the role of convexity in more detail in Section 7. Even when \mathbf{P} is not necessarily convex, we keep using the notation $S_{\mathbf{P}}$ to denote the point defined in the statement of Theorem 5, if and when it exists. We find it natural to call this $S_{\mathbf{P}}$ the *hyperbolic barycenter* of \mathbf{P} .

As in [4, Section 2.1], we say that two ideal polygons \mathbf{P} and \mathbf{Q} are α -related if the cross-ratio $[p_t, q_t, p_{t+1}, q_{t+1}] = \alpha$ for each t , with the convention that the polygons have mutually orthogonal sides when $\alpha = -1$. Note that \mathbf{P} and \mathbf{Q} are α -related (for some α) if and only if the hyperbolic angles between the corresponding sides of \mathbf{P} and \mathbf{Q} are all equal.

Theorem 7. *If two ideal polygons \mathbf{P} and \mathbf{Q} are α -related for some $\alpha \in \mathbb{R}$, then $S_{\mathbf{P}} = S_{\mathbf{Q}}$.*

Proof. By [4, Thm. 16], the values of I, J, K in (3.2) coincide for α -related polygons. \square

Remark 8. Theorem 7 can also be seen in [4] from a complementary point of view. The barycenter of an ideal hyperbolic polygon is *defined* in [4, Section 6.2.1] to be the limit as $\varepsilon \rightarrow 0$ of the fixed point of the composition $L_{1+\varepsilon}(\mathbf{P})$ of infinitesimal rotations along the sides of the polygon \mathbf{P} – let us temporarily denote this point $\check{S}_{\mathbf{P}}$. As explained in [4, Remark 6.9], the Möbius invariance of $IK - J^2$ (cf. [4, Lemma 6.6]) implies $\check{S}_{\mathbf{P}} = \check{S}_{\mathbf{Q}}$ for α -related \mathbf{P} and \mathbf{Q} . Then in [4, Lemma 6.10] it is shown that $\check{S}_{\mathbf{P}}$ has the same minimization property as the $S_{\mathbf{P}}$ in Theorem 5, thus *a posteriori* $\check{S}_{\mathbf{P}} = S_{\mathbf{P}}$.

In the Euclidean setting, there is an analogous notion to the cross-ratio dynamics considered in [4], called *bicycle correspondence*, which also has a fixed point called *circumcenter of mass* (cf. [18, Section 1, Theorem 5, Remark. 3.3]). The next property of the hyperbolic barycenter $S_{\mathbf{P}}$ resembles the similar Archimedean property of the Euclidean circumcenter of mass [19, Theorem 1].

Lemma 9 (Archimedean property). *If the ideal polygon \mathbf{P} is partitioned along any of its diagonals into ideal polygons \mathbf{Q}_1 and \mathbf{Q}_2 , then*

$$\check{S}_{\mathbf{P}} = \frac{I_{\mathbf{Q}_1} + K_{\mathbf{Q}_1}}{I_{\mathbf{P}} + K_{\mathbf{P}}} \check{S}_{\mathbf{Q}_1} + \frac{I_{\mathbf{Q}_2} + K_{\mathbf{Q}_2}}{I_{\mathbf{P}} + K_{\mathbf{P}}} \check{S}_{\mathbf{Q}_2}. \tag{3.5}$$

Proof. Indeed, letting $\mathbf{Q}_1 = (p_1, \dots, p_r)$ and $\mathbf{Q}_2 = (p_1, p_r, \dots, p_n)$, we have

$$I_{\mathbf{P}} = \left(\sum_{t=1}^{r-1} \frac{1}{p_t - p_{t+1}} + \frac{1}{p_r - p_1} \right) + \left(\frac{1}{p_1 - p_r} + \sum_{t=r}^n \frac{1}{p_t - p_{t+1}} \right) = I_{\mathbf{Q}_1} + I_{\mathbf{Q}_2}.$$

Similarly, $J_{\mathbf{P}} = J_{\mathbf{Q}_1} + J_{\mathbf{Q}_2}$ and $K_{\mathbf{P}} = K_{\mathbf{Q}_1} + K_{\mathbf{Q}_2}$, and (3.5) follows from (3.3). □

The basic computation in the proof of the above Lemma 9 admits the following dynamical interpretation (cf. Remark 8). Since the infinitesimal rotation along the (oriented) side $\xi(p_t, p_{t+1})$ is given by the Minkowski cross-product with the principal polar ξ_t^* , and the principal polars $\xi^*(p_1, p_r)$ and $\xi^*(p_r, p_1)$ have opposite signs, the corresponding inputs in the composition of such infinitesimal rotations cancel each other. Moreover, Lemma 9 admits also the following useful geometric consequence.

Corollary 10. *With notation as in Lemma 9, the hyperbolic barycenters $S_{\mathbf{P}}$, $S_{\mathbf{Q}_1}$, and $S_{\mathbf{Q}_2}$ lie on a common geodesic.*

Proof. $\check{S}_{\mathbf{P}}$ is a weighted sum of $\check{S}_{\mathbf{Q}_1}$ and $\check{S}_{\mathbf{Q}_2}$ with weights summing to 1, so they are collinear. □

Remark 11. Relative to the hyperboloid model, (3.5) in Lemma 9 becomes

$$\hat{S}_{\mathbf{P}} = \sqrt{\frac{I_{\mathbf{Q}_1} K_{\mathbf{Q}_1} - J_{\mathbf{Q}_1}^2}{I_{\mathbf{P}} K_{\mathbf{P}} - J_{\mathbf{P}}^2}} \cdot \hat{S}_{\mathbf{Q}_1} + \sqrt{\frac{I_{\mathbf{Q}_2} K_{\mathbf{Q}_2} - J_{\mathbf{Q}_2}^2}{I_{\mathbf{P}} K_{\mathbf{P}} - J_{\mathbf{P}}^2}} \cdot \hat{S}_{\mathbf{Q}_2}. \tag{3.6}$$

The expression $I_{\mathbf{P}} K_{\mathbf{P}} - J_{\mathbf{P}}^2$ plays a prominent role in the study of cross-ratio dynamics of general ideal polygons (see in particular [4, Section 6]). We presume it should be possible to show within that framework that this Casimir function is always strictly positive, at least for convex \mathbf{P} . However, having now established the theoretical foundation of our study of hyperbolic barycenters with Theorem 5, we find it more convenient to work from now on in the Beltrami–Cayley–Klein model, in which our remaining considerations become simpler to state and prove (see also Remark 12 below).

Corollary 10 leads immediately to the recursive geometric construction of the hyperbolic barycenters of arbitrary convex ideal hyperbolic polygons, starting from symmedian points of triangles by Theorem 4 and the classical construction in Figure 1 (see the next Section 4). There is another method to construct hyperbolic barycenters geometrically. Motivated by the

dynamical interpretation of the point $S_{\mathbf{P}}$ of Theorem 5 as the fixed point in \mathbb{H} of the composition of infinitesimal rotations along all the sides of \mathbf{P} , we may consider more generally the fixed point of the composition of those infinitesimal rotations along any sequence of sides of \mathbf{P} , as follows.

For $\Xi = \{\xi_{t_1}, \dots, \xi_{t_k}\}$ a non-empty set of (not necessarily contiguous) sides of \mathbf{P} , with principal polars $\check{\xi}_t^* = (I_t + K_t, I_t - K_t, 2J_t)$ as in (2.5) and (3.1), let us write analogously as in (3.2) and (3.3):

$$I_{\Xi} := \sum_{\xi_t \in \Xi} I_t; \quad J_{\Xi} := \sum_{\xi_t \in \Xi} J_t; \quad K_{\Xi} := \sum_{\xi_t \in \Xi} K_t; \quad \text{and} \quad \check{S}_{\Xi} := \left(\frac{I_{\Xi} - K_{\Xi}}{I_{\Xi} + K_{\Xi}}, \frac{2J_{\Xi}}{I_{\Xi} + K_{\Xi}} \right). \quad (3.7)$$

Remark 12. The point S_{Ξ} need not be in \mathbb{H} . For example, $\check{S}_{\{\xi\}}$ is the polar $\check{\xi}^*$ to ξ , which is outside of the unit disk, and $\check{S}_{\{\xi_1, \xi_2\}} = \left(\frac{1-p_2^2}{1+p_2^2}, \frac{2p_2}{1+p_2^2} \right) =: \check{P}_2$ is the common ideal vertex of the sides $\xi_1 = \xi(p_1, p_2)$ and $\xi_2 = \xi(p_2, p_3)$, which lies on the absolute \mathbf{O} . Mainly on account of these two basic examples, we prefer to work with the gnomonic projections S_{Ξ} to the Beltrami–Cayley–Klein plane $x_0 = 1$ than in the wider ambient Minkowski space $\mathbb{R}^{2,1}$.

We set aside a more systematic discussion of the geometric meaning of \check{S}_{Ξ} for arbitrary Ξ , in favor of focusing on the most immediately relevant configuration properties of the points S_{Ξ} for different interrelated choices of Ξ , after introducing some useful notation. For $\Xi = \{\Xi_1, \dots, \Xi_v\}$ a finite collection of non-empty sets Ξ_s of sides of \mathbf{P} as above, and given a side ξ_t of \mathbf{P} , we denote by $\mu_{\Xi}(\xi_t)$ the multiplicity of ξ_t in the multiset sum of the $\Xi_s \in \Xi$.

Lemma 13 (Interpolation Lemma). *Let $\Xi = \{\Xi_1, \dots, \Xi_v\}$, where the Ξ_s are non-empty sets of sides of \mathbf{P} , such that $I_{\Xi} + K_{\Xi} := \sum_{s=1}^v (I_{\Xi_s} + K_{\Xi_s}) \neq 0$, with notation as in (3.7). Denote*

$$\check{S}_{\Xi} := \sum_{s=1}^v \frac{I_{\Xi_s} + K_{\Xi_s}}{I_{\Xi} + K_{\Xi}} \cdot \check{S}_{\Xi_s}. \quad (3.8)$$

If all the multiplicities $\mu_{\Xi}(\xi_t) = m$, for some $m \in \mathbb{N}$ independent of $t = 1, \dots, n$, then $\check{S}_{\Xi} = \check{S}_{\mathbf{P}}$.

Proof. We see from (3.7) that each $(I_{\Xi_s} + K_{\Xi_s}) \cdot \check{S}_{\Xi_s} = (I_{\Xi_s} - K_{\Xi_s}, 2J_{\Xi_s})$ – this is so even in the exceptional case where $I_{\Xi_s} + K_{\Xi_s} = 0$, but then only by convention. Thus

$$\sum_{s=1}^v (I_{\Xi_s} + K_{\Xi_s}) \cdot \check{S}_{\Xi_s} = m \cdot (I_{\mathbf{P}} + K_{\mathbf{P}}) \cdot \check{S}_{\mathbf{P}},$$

and similarly $I_{\Xi} + K_{\Xi} = m \cdot (I_{\mathbf{P}} + K_{\mathbf{P}})$, whence our result is immediate. □

Lemma 13 will be one of the main tools that allows for the geometric construction of hyperbolic barycenters (see the next Section 4), mainly through the following immediate consequence.

Corollary 14. *If \mathbf{P} is convex and $\Xi = \{\Xi_1, \dots, \Xi_v\}$, where the Ξ_s are sets of sides of \mathbf{P} with $|\Xi_s| \geq 2$ and such that $I_{\Xi} + K_{\Xi} \neq 0$, then S_{Ξ} as in (3.8) lies in the convex hull of the S_{Ξ_s} .*

Proof. The weights $\frac{I_{\Xi_s} + K_{\Xi_s}}{I_{\Xi} + K_{\Xi}}$ are all positive (cf. Remark 6) and sum to 1. □

It is educational to begin to see these results in action in some trivial cases. For any ideal n -gon \mathbf{P} , we can take $\Xi = \{\Xi_1, \dots, \Xi_n\}$, where $\Xi_t = \{\xi_{t-1}, \xi_t\}$, the two sides that meet at the ideal vertex on $\ell(p_t)$, which is precisely S_{Ξ_t} (cf. Remark 12). We see from the computation in the proof of Lemma 13 that the hypothesis that $I_{\Xi} + K_{\Xi} = m \cdot (I_{\mathbf{P}} + K_{\mathbf{P}}) \neq 0$ is redundant in case \mathbf{P} is convex, by Remark 6. In this case we also witness algebraically that $\check{S}_{\Xi} = \check{S}_{\mathbf{P}}$ lies in the interior of \mathbf{P} by Corollary 14, which is neither surprising nor immediately apparent from the algebraic expression (3.3), as we formally record in the following result.

Corollary 15. *If \mathbf{P} is convex then $S_{\mathbf{P}}$ lies in the interior of \mathbf{P} .*

In the tired case of triangles $\mathbf{P} = (p_1, p_2, p_3)$, fix $t \in \{1, 2, 3\}$ and let $\Xi_1 = \{\xi_t\}$ and $\Xi_2 = \{\xi_{t-1}, \xi_{t+1}\}$. Then \check{S}_{Ξ_1} is the polar $\check{\xi}_t^*$ to ξ_t , and \check{S}_{Ξ_2} is the ideal vertex \check{P}_t on $\ell(p_t)$ (cf. (2.4)) where the other two sides meet (cf. Remark 12). Thus Corollary 14 says in this case that $\check{S}_{\mathbf{P}} = \check{S}_{\{\Xi_1, \Xi_2\}}$ lies on the hyperbolic altitude from \check{P}_t , as expected (cf. Theorem 2). A first non-trivial consequence of Corollary 14 is that this argument works all the same even if the first and third sides do not meet to form a triangle, as formalized in the following result.

Lemma 16. *Let $\Xi = \{\check{\xi}_{t-1}, \xi_t, \check{\xi}_{t+1}\}$ be any set of three consecutive sides. Then S_{Ξ} is the intersection of the two hyperbolic altitudes, from \check{P}_t to $\check{\xi}_{t+1}^*$, and from \check{P}_{t+1} to $\check{\xi}_{t-1}^*$.*

Proof. Partition Ξ in two different ways: $\Xi_1 = \{\Xi_{11}, \Xi_{12}\}$ and $\Xi_2 = \{\Xi_{21}, \Xi_{22}\}$, where $\Xi_{11} = \{\xi_{t-1}\}$ and $\Xi_{12} = \{\xi_t, \xi_{t+1}\}$, and $\Xi_{21} = \{\xi_{t+1}\}$ and $\Xi_{22} = \{\xi_{t-1}, \xi_t\}$. Then an analogous computation to that in the proof of Lemma 13 yields immediately that $\check{S}_{\Xi_1} = \check{S}_{\Xi} = \check{S}_{\Xi_2}$, whence \check{S}_{Ξ} lies on both geodesic segments $\check{S}_{\Xi_{11}}\check{S}_{\Xi_{12}}$ and $\check{S}_{\Xi_{21}}\check{S}_{\Xi_{22}}$ by Corollary 14. To conclude, we observe as in Remark 12 that $\check{S}_{\Xi_{11}} = \check{\xi}_{t-1}^*$ and $\check{S}_{\Xi_{12}} = \check{P}_{t+1}$, and $\check{S}_{\Xi_{21}} = \check{\xi}_{t+1}^*$ and $\check{S}_{\Xi_{22}} = \check{P}_t$. \square

Remark 17. Lemma 16 is the third in a recursive series of constructions initiated in Remark 12. For $\Xi = \{\xi_0, \dots, \xi_t\}$ a set of $t + 1$ consecutive sides, we find that \check{S}_{Ξ} is the intersection of the geodesic segments $\check{\xi}_0^*\check{S}_{\Xi_0}$ and $\check{S}_{\Xi_t}\check{\xi}_t^*$, where $\Xi_s := \Xi - \{\xi_s\}$. More generally, the geodesic segments $\check{S}_{\{\xi_0, \dots, \xi_{s-1}\}}\check{S}_{\{\xi_s, \dots, \xi_t\}}$ for $s = 1, \dots, t$ are all concurrent at \check{S}_{Ξ} . Moreover, if we further assume that these are sides of a convex ideal polygon, then the same computation as in Theorem 5 yields that this \check{S}_{Ξ} also minimizes the sum of the hyperbolic sines of the hyperbolic distances to the sides in Ξ .

4. Case studies: small-gons

Lemma 9, Lemma 13, and their corollaries established in Section 3, are especially useful for geometrically constructing the hyperbolic barycenters of ideal hyperbolic n -gons recursively. Since we have already extensively addressed the particular case of triangles, let us now illustrate these constructions in the next few particular cases of $n = 4, 5, 6, 10$, where we begin to glimpse a cascade of concurrences culminating at the hyperbolic barycenter. In order to be better able to illustrate our constructions with figures, we shall work exclusively within the Beltrami–Cayley–Klein model from now on, and drop the notation \check{S} introduced in Remark 3, whose purpose was to help disambiguate between this and the hyperboloid model.

4.1. Case study: Quadrilaterals

A first construction of the hyperbolic barycenter of an ideal quadrilateral \mathbf{P} (and in general, of an ideal polygon) is achieved via the Archimedean Property recursively from the case of triangles (and in general, from the case of smaller-gons). Let S_t be the symmedian point of the triangle $\Delta(P_{t-1}P_tP_{t+1})$. Then by Corollary 10 $S_{\mathbf{P}}$ lies on S_1S_3 and on S_2S_4 (see Figure 4).

Surprisingly, an alternative construction makes it easier to construct hyperbolic barycenters of ideal quadrilaterals than those of ideal triangles, as we see in the next result.

Theorem 18. *The hyperbolic barycenter of an ideal quadrilateral \mathbf{P} lies on its diagonals.*

Proof. Let $\Xi_t := \{\xi_{t-1}, \xi_t\}$ denote the set of sides meeting at the ideal vertex P_t , where as usual we take indices modulo $n = 4$. With notation as in (3.7), we see that each $S_{\Xi_t} = P_t$ (cf. Remark 12). Letting also $\Xi_o := \{\Xi_1, \Xi_3\}$ and $\Xi_e := \{\Xi_2, \Xi_4\}$, we obtain from Lemma 13 that $S_{\Xi_o} = S_{\mathbf{P}} = S_{\Xi_e}$. Finally, it follows from Corollary 14 that $S_{\Xi_o} = S_{\mathbf{P}}$ lies on the geodesic segment $S_{\Xi_1}S_{\Xi_3} = P_1P_3$, and similarly $S_{\Xi_e} = S_{\mathbf{P}}$ lies on the geodesic segment $S_{\Xi_2}S_{\Xi_4} = P_2P_4$. \square

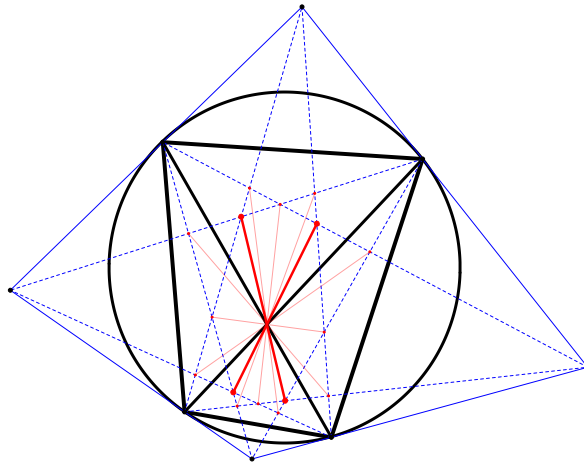


Figure 4. The hyperbolic barycenter of an ideal quadrilateral is the intersection point of its diagonals as well as the intersection of the segments connecting symmedians of opposite triangles in each triangulation.

Corollary 19. *The hyperbolic barycenter of an ideal quadrilateral \mathbf{P} is the intersection of the diagonals $\xi_1^* \xi_3^*$ and $\xi_2^* \xi_4^*$, of the quadrilateral formed by the polars to the sides.*

Proof. This is an immediate consequence of Theorem 18 and the well-known (Euclidean!) fact [3, Section 11.1.7] that the diagonals of a circumscribed quadrilateral intersect at the same point as the diagonals of the inscribed quadrilateral whose vertices are the points of tangency. \square

The trivial observation in Corollary 19 has the non-trivial consequence in Lemma 20 below.

Lemma 20. *The hyperbolic barycenter of an ideal quadrilateral simultaneously and independently minimizes the sum of hyperbolic sines of hyperbolic distances to each pair of opposite sides.*

Proof. Let $\Xi_o := \{\xi_1, \xi_3\}$ and $\Xi_e := \{\xi_2, \xi_4\}$. The same computation as in the proof of Theorem 5 shows that S_{Ξ_o} (resp., S_{Ξ_e}) minimizes the sum of the hyperbolic sines of the hyperbolic distances to ξ_1 and ξ_3 (resp., ξ_2 and ξ_4). Writing $\Xi_{\text{odd}} = \{\{\xi_1\}, \{\xi_3\}\}$ and $\Xi_{\text{even}} = \{\{\xi_2\}, \{\xi_4\}\}$, we see as in Lemma 13 that $S_{\Xi_{\text{odd}}} = S_{\Xi_o}$ and $S_{\Xi_{\text{even}}} = S_{\Xi_e}$, whence by Corollary 14 S_{Ξ_o} lies on $\xi_1^* \xi_3^*$ and S_{Ξ_e} lies on $\xi_2^* \xi_4^*$ (cf. Remark 12). Letting $\Xi_{\text{tot}} = \{\Xi_o, \Xi_e\}$, then $S_{\Xi_{\text{tot}}} = S_{\mathbf{P}}$ again by Lemma 13, whence again by Corollary 14 $S_{\mathbf{P}}$ lies on the geodesic segment $S_{\Xi_o} S_{\Xi_e}$. Since $S_{\mathbf{P}}$ is the intersection of $\xi_1^* \xi_3^*$ and $\xi_2^* \xi_4^*$ by Corollary 19, this forces S_{Ξ_o} to also lie on $\xi_2^* \xi_4^*$ and S_{Ξ_e} to also lie on $\xi_1^* \xi_3^*$. \square

Remark 21. The anonymous referee has made the interesting observation that many of the concurrences that we have seen so far are limiting cases of the infamous Brianchon Theorem [3, Section 11.1.5]. First, the original construction of the symmedian point of a triangle in Figure 1 is the Brianchon concurrence for the degenerate “hexagon” $AB^*CA^*BC^*$. Next, the Euclidean fact [3, Section 11.1.7] used in the proof of Corollary 19 is similarly obtained from the two degenerate “hexagons” containing the four polars and one pair of opposite vertices of the ideal quadrilateral.

Besides the two constructions of the hyperbolic barycenter $S_{\mathbf{P}}$ of an ideal quadrilateral \mathbf{P} , we witness in Figure 4 many additional concurrences at $S_{\mathbf{P}}$, some more of which can be seen as limiting cases of Brianchon’s Theorem, which we leave unaddressed as exercises for the interested reader.

4.2. Case study: Pentagons

Our first construction of the hyperbolic barycenter of an ideal pentagon \mathbf{P} is obtained from the Archimedean Property. Let S_t be the symmedian point of the triangle $\Delta(P_{t-1}P_tP_{t+1})$, and let T_t be the intersection of the two diagonals not containing P_t : $P_{t-1}P_{t+2}$ and $P_{t+1}P_{t-2}$. Then by Theorem 18, T_t is the hyperbolic barycenter of the quadrilateral $P_{t-2}P_{t-1}P_{t+1}P_{t+2}$. Thus by Corollary 10, the five geodesic segments S_tT_t are concurrent at $S_{\mathbf{P}}$. On the other hand, we can use the Interpolation Lemma to provide an alternative construction of the hyperbolic barycenter $S_{\mathbf{P}}$.

Lemma 22. *Let \mathbf{P} be a convex ideal hyperbolic pentagon. Let R_t be the intersection of the two hyperbolic altitudes, from the vertex P_{t+2} to the side $P_{t-2}P_{t-1}$, and from the vertex P_{t-2} to the side $P_{t+1}P_{t+2}$, i.e., R_t lies on $P_{t+2}\xi_{t+3}^*$ and on $P_{t+3}\xi_{t+1}^*$. Then the hyperbolic barycenter $S_{\mathbf{P}}$ lies on the geodesic segment P_tR_t .*

Proof. By Corollary 14 applied to $\Xi = \{\Xi_1, \Xi_2\}$, with $\Xi_1 = \{\xi_{t-1}, \xi_t\}$ and $\Xi_2 = \{\xi_{t+1}, \xi_{t+2}, \xi_{t+3}\}$, $S_{\Xi} = S_{\mathbf{P}}$ lies on $S_{\Xi_1}S_{\Xi_2}$. Now $S_{\Xi_1} = P_t$ (cf. Remark 12), and $S_{\Xi_2} = R_t$ by Lemma 16. \square

We witness in Figure 5 that in the case of ideal pentagons also, as in the case of ideal quadrilaterals, the hyperbolic barycenter is at the epicenter of several kinds of concurrences.

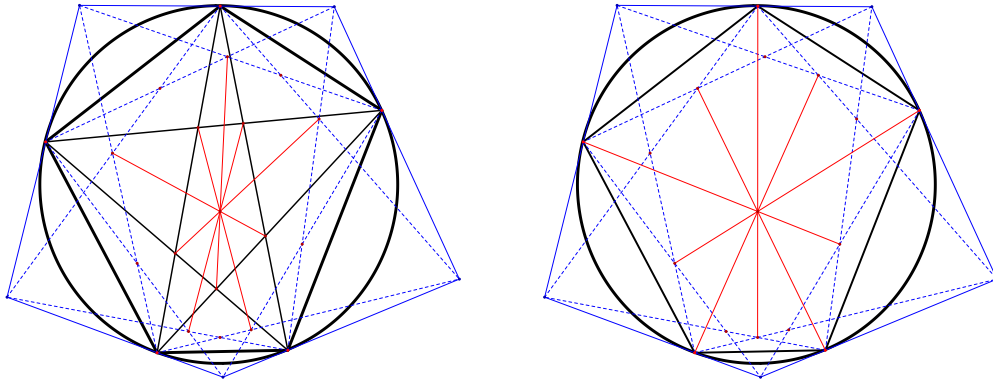


Figure 5. Constructions of the hyperbolic barycenter of an ideal pentagon. Left: via the Archimedean property. Right: via the Interpolation Lemma.

4.3. Case study: Hexagons

Surprisingly, it is relatively easier to construct the hyperbolic barycenter of an ideal hexagon than that of an ideal pentagon. In fact, the construction of the former arises from one of the variants of the Brianchon Theorem (see [3, Section 11.1.9] and Figure 6; see also Remark 21).

Theorem 23. *Let \mathbf{Q} be the hexagon in \mathbb{H} whose sides lie on the short diagonals of the ideal hexagon \mathbf{P} . Then the long diagonals of \mathbf{Q} all intersect at $S_{\mathbf{P}}$.*

Proof. For each t , consider the ideal quadrilateral $(p_{t-1}, p_t, p_{t+1}, p_{t+2})$, and let Q_t be its hyperbolic barycenter. By Theorem 18, Q_t is the intersection point of P_tP_{t+2} and $P_{t-1}P_{t+1}$, and by Corollary 9, $S_{\mathbf{P}}$ lies on the geodesic segment Q_tQ_{t+3} . \square

Another construction of the hyperbolic barycenter of an ideal hexagon is obtained from the Interpolation Lemma, as follows. Let R_t be the intersection of $P_tP_{t+1}^*$ and $P_{t+1}P_{t-1}^*$. Then $R_t = S_{\Xi_t}$ for $\Xi_t := \{\xi_{t-1}, \xi_t, \xi_{t+1}\}$ by Lemma 16. Applying Corollary 14 to $\Xi = \{\Xi_t, \Xi_{t+3}\}$, we find that $S_{\mathbf{P}}$ lies on each geodesic segment R_tR_{t+3} .

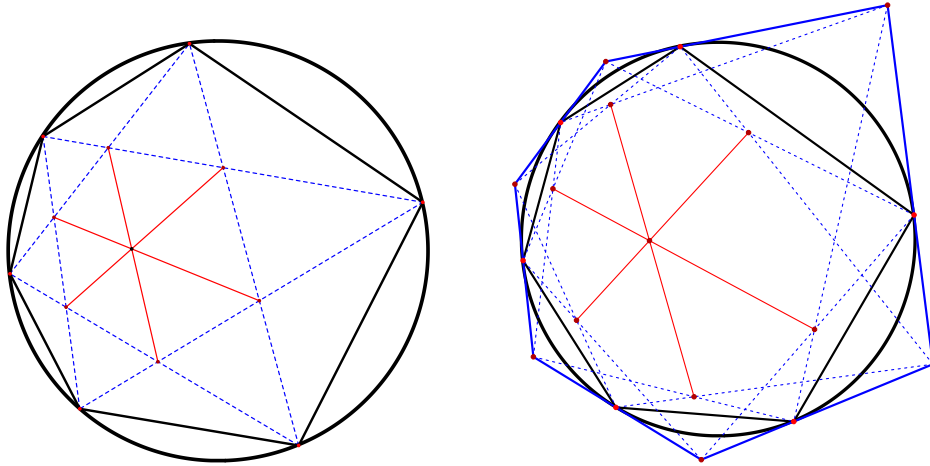


Figure 6. Constructions of the hyperbolic barycenter of an ideal hexagon. Left: via the Archimedean property. Right: via the Interpolation Lemma.

4.4. *Case study: $(2^m + 2)$ -gons*

The (initially surprising) relative simplicity in the construction of hyperbolic barycenters for ideal hexagons versus ideal pentagons is part of a general phenomenon, which leads to a layered family of interesting concurrences arising from the Archimedean Property. We can subdivide an ideal $(2^m + 2)$ -gon \mathbf{P} along any of its $2^{m-1} + 1$ long diagonals into two $(2^{m-1} + 2)$ -gons \mathbf{Q}_1 and \mathbf{Q}_2 , and conclude by Corollary 10 that $S_{\mathbf{P}}$ lies on $S_{\mathbf{Q}_1} S_{\mathbf{Q}_2}$. This gives a concurrence of $2^{m-1} + 1$ lines, each of whose endpoints is itself a concurrence of $2^{m-2} + 1$ lines, each of whose endpoints is itself a concurrence \dots , etc. This recursively reduces the construction of $S_{\mathbf{P}}$ to any one of the many equivalent constructions of the hyperbolic barycenter of an ideal quadrilateral in Section 4.1 (see Figure 4). In Figure 7 we depict the next case $m = 3$ of this construction, to obtain the hyperbolic barycenter of an ideal decagon as the point of concurrence of the five line segments connecting opposite hyperbolic barycenters of ideal hexagons constructed according to Theorem 23.

5. Moduli of ideal polygons with fixed hyperbolic barycenter

Let us denote by $\mathcal{M}_n(S) = \mathcal{M}_n(\alpha, \beta)$ the moduli space of ideal n -gons having a fixed $S = (\alpha, \beta) \in \mathbb{H}$ as their hyperbolic barycenter. We immediately see from the coordinatization of $S_{\mathbf{P}}$ in (3.3) that

$$\begin{cases} I_{\mathbf{P}} - K_{\mathbf{P}} = \alpha \cdot (I_{\mathbf{P}} + K_{\mathbf{P}}); \\ 2J_{\mathbf{P}} = \beta \cdot (I_{\mathbf{P}} + K_{\mathbf{P}}) \end{cases} \tag{5.1}$$

defines a subspace of codimension at most 2 in the moduli space \mathcal{P}_n of ideal hyperbolic n -gons. We would like to have a more geometrically meaningful description of $\mathcal{M}_n(S)$ than merely the algebraic conditions in (5.1). Here we accomplish this only for the smallest values of $n = 3, 4$.

5.1. *Moduli of ideal triangles with fixed hyperbolic barycenter*

The space \mathcal{P}_3 of all ideal hyperbolic triangles is three-dimensional, hence the subspaces $\mathcal{M}_3(S)$ are expected to be one-dimensional. It is clear from the minimality property of $S_{\mathbf{P}}$ in Theorem 5 that all the triangles obtained from \mathbf{P} by a hyperbolic rotation about $S_{\mathbf{P}}$ share the same hyperbolic barycenter, yielding a one-dimensional family, as expected. It is easy to see that this is indeed all of $\mathcal{M}_3(S_{\mathbf{P}})$, as we show next.

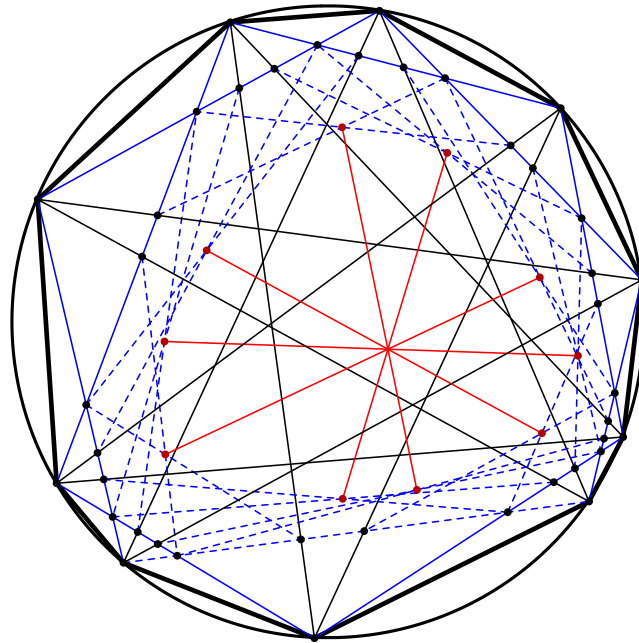


Figure 7. Recursive construction of the hyperbolic barycenter of an ideal decagon.

Lemma 24. *Two ideal triangles \mathbf{P}_1 and \mathbf{P}_2 share the same hyperbolic barycenter $S_{\mathbf{P}_1} = S = S_{\mathbf{P}_2}$ if and only if they are obtained from one another by a hyperbolic rotation about S .*

Proof. It suffices to show that if an ideal triangle $\mathbf{P} = (p_1, p_2, p_3)$ has $S_{\mathbf{P}} = (0, 0)$ then it is regular. This follows from a simple algebraic computation. If we rotate such a triangle so that one of its vertices is at $0 \in \mathbb{R}\mathbb{P}^1$, say $p_3 = 0$, then $2J_{\mathbf{P}} = 0$ if and only if $p_1 + p_2 = 0$, and $I_{\mathbf{P}} - K_{\mathbf{P}} = 0$ if and only if $p_1^2 p_2^2 - p_1 p_2 - (p_1 - p_2)^2 = 0$, which together imply $\{p_1, p_2\} = \{\pm\sqrt{3}\}$, as required. \square

An alternative construction of $\mathcal{M}_3(S)$ is as follows. Given an ideal hyperbolic triangle \mathbf{P} , consider the ideal hyperbolic triangle $\tilde{\mathbf{P}}$, whose ideal vertex \tilde{P}_t is the hyperbolic reflection of P_t with respect to its opposite side $\xi_{t+1} = P_{t+1}P_{t+2}$. Then the points P_t, \tilde{P}_t , and ξ_{t+1}^* are collinear by construction. Since $S_{\mathbf{P}}$ is the hyperbolic orthocenter of \mathbf{P} , it also lies on $P_t \xi_{t+1}^*$, and by symmetry (since $\tilde{\mathbf{P}} = \mathbf{P}$) we see that $\tilde{\xi}_{t+1}^*$ is also on this line. Hence $S_{\mathbf{P}}$ is the hyperbolic orthocenter of $\tilde{\mathbf{P}}$.

Lemma 25. *The six polars $\xi_1^*, \xi_2^*, \xi_3^*, \tilde{\xi}_1^*, \tilde{\xi}_2^*, \tilde{\xi}_3^*$ all lie on the same conic $\Gamma_{\mathbf{P}}$.*

Proof. Consider the unique conic Γ passing through the first five of these points, except possibly $\tilde{\xi}_3^*$. Then we see that $\xi_1^*, \xi_2^*, \xi_3^*$ form a 3-periodic Poncelet trajectory on Γ circumscribed about \mathbf{O} . By the Poncelet Theorem [9, Theorem. 2.14], the Poncelet trajectory on Γ containing $\tilde{\xi}_1^*$ and $\tilde{\xi}_2^*$ is also 3-periodic, whence $\tilde{\xi}_3^*$ also lies on Γ . \square

Theorem 26. *The moduli space $\mathcal{M}_3(S_{\mathbf{P}})$ consists of the ideal triangles whose ideal vertices are the tangency points of polar triangles circumscribed in the 3-periodic Poncelet pair $(\Gamma_{\mathbf{P}}, \mathbf{O})$, where $\Gamma_{\mathbf{P}}$ is the conic associated in Lemma 25 with \mathbf{P} . The conic $\Gamma_{\mathbf{P}} = \Gamma(S_{\mathbf{P}})$ depends only on $S_{\mathbf{P}}$, and not on \mathbf{P} .*

Proof. After applying an isometry sending S to $(0, 0)$, it suffices to prove this for the special case $S = (0, 0)$, which is an immediate consequence of Lemma 24. \square

In order to find $\Gamma(S)$ explicitly it suffices to find $\Gamma(r, 0)$ for $0 \leq r < 1$, and then rotate by θ to reach any desired $S = (r \cos \theta, r \sin \theta) \in \mathbb{H}$. There are two special triangles \mathbf{P} and $\tilde{\mathbf{P}}$ such that

$S_{\mathbf{p}} = S_{\tilde{\mathbf{p}}} = (r, 0)$ with $p_3 = 0$ and $\tilde{p}_3 = \infty$, respectively. We find $p_1 + p_2 = 0 = \tilde{p}_1 + \tilde{p}_2$ (from $J = 0$), and then that $p_1 = \pm\sqrt{3\frac{1-r}{1+r}}$ and $\tilde{p}_1 = \frac{-p_1}{3}$ (from $I - J = r(I + J)$). We then compute from (2.5) (projected down to the Beltrami–Cayley–Klein model) that

$$\xi_1^* = \left(\frac{r-2}{1-2r}, 0\right); \quad \xi_2^* = (1, -p_1); \quad \xi_3^* = (1, p_1); \quad \tilde{\xi}_1^* = \left(\frac{r+2}{2r+1}, 0\right); \quad \tilde{\xi}_2^* = (-1, 3p_1^{-1}); \quad \tilde{\xi}_3^* = (-1, -3p_1^{-1}).$$

It is trivial to verify that

$$\Gamma(r, 0) : (1 - 4r^2)x_1^2 + 6rx_1 + (1 - r^2)x_2^2 + r^2 - 4 = 0$$

is the unique (overdetermined!) conic passing through all six polars as in Lemma 25. The following amusing observation is then immediate.

Corollary 27. *The Poncelet conic $\Gamma(S)$ is an ellipse (resp., a parabola; resp., a hyperbola) if and only if $|S| < 1/2$ (resp., $|S| = 1/2$; resp., $|S| > 1/2$), where $|S|$ denotes the Euclidean norm of S .*

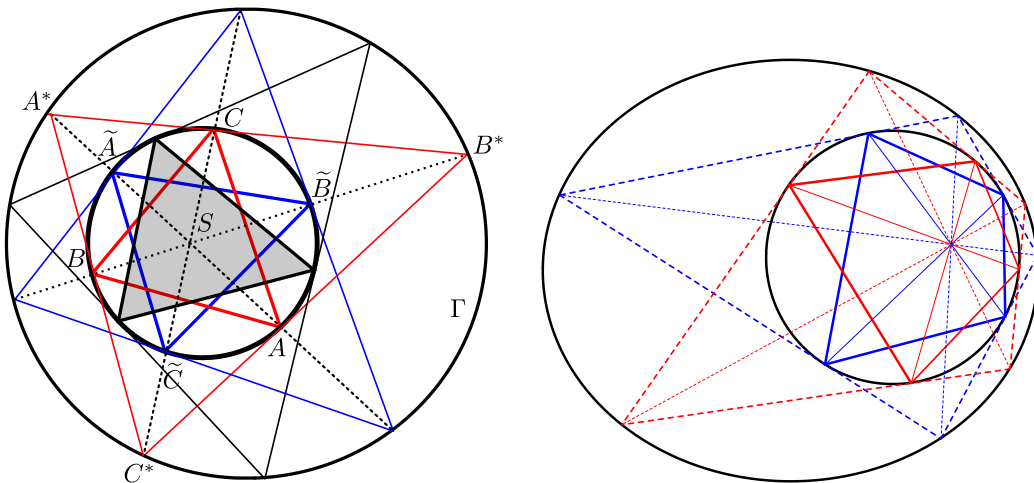


Figure 8. Left: Poncelet conic of all ideal triangles with a common hyperbolic barycenter. Right: one representative of the pencil of Poncelet conics of ideal quadrilaterals with a common hyperbolic barycenter.

5.2. Moduli of ideal quadrilaterals with fixed hyperbolic barycenter

The space \mathcal{P}_4 of all ideal hyperbolic quadrilaterals is four-dimensional, hence the subspaces $\mathcal{M}_4(S)$ are expected to be two-dimensional. Theorem 18 immediately yields a compact and satisfying description of $\mathcal{M}_4(S)$: choose any two distinct hyperbolic lines δ_1 and δ_2 intersecting at S to be the diagonals of the arbitrary ideal quadrilateral \mathbf{P} with $S_{\mathbf{p}}$. This construction exhausts all of $\mathcal{M}_4(S)$, and is roughly analogous to our first description of $\mathcal{M}_3(S)$ in terms of rotations about S in Lemma 24. Inspired by the description of $\mathcal{M}_3(S)$ in terms of Poncelet conics afforded by Theorem 26, we seek a similar description of $\mathcal{M}_4(S)$.

Given an ideal hyperbolic quadrilateral \mathbf{P} , its four polars ξ_t^* determine a pencil $\Gamma_{\mathbf{p}}$ of conics passing through these four points. For a generic fifth point Q , let $\Gamma_{\mathbf{p}}(Q)$ be the unique conic on this pencil that also passes through Q . Then $(\Gamma_{\mathbf{p}}(Q), \mathbf{O})$ forms a 4-periodic Poncelet pair, whence by the Poncelet Theorem [9, Theorem 2.14] $Q = \tilde{\xi}_1^*$ is polar to the side of a unique ideal quadrilateral $\tilde{\mathbf{P}}$ all of whose polars $\tilde{\xi}_t^*$ are also on $\Gamma_{\mathbf{p}}(Q)$. It is not obvious (and for us, not even

expected) that we should always have $S_{\mathbf{P}} = S_{\mathbf{P}}$ as apparently depicted in Figure 8. In the next result we show that this is indeed the case, and that this construction exhausts all of $\mathcal{M}_4(S_{\mathbf{P}})$.

Theorem 28. *The moduli space $\mathcal{M}_4(S_{\mathbf{P}})$ consists of the ideal quadrilaterals whose ideal vertices are the tangency points of polar quadrilaterals circumscribed in a 4-periodic Poncelet pair (Γ, \mathbf{O}) , for some conic Γ in the pencil $\Gamma_{\mathbf{P}}$.*

Proof. After applying an isometry sending S to $(0, 0)$, it suffices to prove this for the special case $S = (0, 0)$. By Corollary 19, it suffices to prove the claim that for any $\mathbf{P} \in \mathcal{M}_4(0, 0)$, any Γ in $\Gamma_{\mathbf{P}}$, and any \mathbf{Q}^* circumscribed in (Γ, \mathbf{O}) , the diagonals of \mathbf{Q}^* intersect at the origin.

To prove the claim, first note that $S_{\mathbf{P}} = (0, 0)$ if and only if \mathbf{P} is a rectangle, which after a harmless rotation about the origin may be assumed to have its sides parallel to the coordinate axes. Then the polar quadrilateral $\mathbf{P}^* = \xi_1^* \xi_2^* \xi_3^* \xi_4^*$ is a rhombus whose vertices lie on the coordinate axes. By comparing the general form of a conic evaluated at each pair ξ_t^* and ξ_{t+2}^* , we discover immediately that every (non-degenerate) Γ in the pencil $\Gamma_{\mathbf{P}}$ must be a central ellipse. Our claim follows immediately from the following general Lemma 29. \square

We have severed the following configuration result from the rest of the proof of Theorem 28 due to its independent interest. We provide a short conceptual proof because we have not found a reference for it in the literature, even though it is surely well-known to the experts.

Lemma 29. *If Γ is a central ellipse such that (Γ, \mathbf{O}) forms a 4-periodic Poncelet pair then every circumscribed polygon in (Γ, \mathbf{O}) is a rhombus centered at the origin.*

Proof. Let us first show this in the special case where our circumscribed \mathbf{Q} has one of its vertices, call it Q_1 , on a vertex of Γ . Begin constructing the Poncelet orbit in both directions starting from Q_1 , to obtain Q_2 and Q_4 . By symmetry, these are both the next vertices of the ellipse (as we claim), or both in the hemisphere containing Q_1 , or both in the hemisphere containing $-Q_1$. We see again by symmetry that the latter two impossibilities would contradict the 4-periodicity of the Poncelet pair (Γ, \mathbf{O}) .

We can assume without loss of generality that the axes of Γ coincide with the coordinate axes. We ignore from now on the special case already established above. Let us label the vertices of any other \mathbf{Q} circumscribed in (Γ, \mathbf{O}) such that Q_t lies on the t -th quadrant. For any other such $\tilde{\mathbf{Q}} \neq \mathbf{Q}$ circumscribed in (Γ, \mathbf{O}) , the vertex \tilde{Q}_t in the t -th quadrant lies before (resp., after) Q_t , relative to the standard counterclockwise orientation of Γ , for all t simultaneously. Suppose that Q_3 lies before (resp., after) $-Q_1$ for some \mathbf{Q} , contrary to our contention. Then every vertex of \mathbf{Q} lies before (resp., after) every vertex of $-\mathbf{Q}$. But this would imply, by symmetry, that every vertex of $-\mathbf{Q}$ must lie before (resp., after) every vertex of $-(-\mathbf{Q}) = \mathbf{Q}$, which is absurd. \square

Remark 30. We see from Theorem 28 that for any two ideal quadrilaterals $\mathbf{P} \neq \mathbf{Q}$ such that $S_{\mathbf{P}} = S_{\mathbf{Q}}$, the eight distinct polars of \mathbf{P} and \mathbf{Q} belong to the same conic, which is in fact the unique common conic to both pencils $\Gamma_{\mathbf{P}}$ and $\Gamma_{\mathbf{Q}}$.

In the case of triangles, $\mathcal{M}_3(S_{\mathbf{P}})$ is triply covered by the conic $\Gamma_{\mathbf{P}}$ traced out by the polars of the triangles obtained by rotating \mathbf{P} about $S_{\mathbf{P}}$. This exceptional phenomenon does not occur in general for ideal quadrilaterals \mathbf{P} , with an important exception. After an isometry sending $S_{\mathbf{P}}$ to the origin, we see that the polars of the rotations of \mathbf{P} about $S_{\mathbf{P}}$ in general trace out two disjoint conics corresponding to pairs of opposite sides. These two conics coincide precisely when \mathbf{P} is harmonic, which case we begin to study systematically in the next section.

6. Least-squares points and harmonic polygons

Thus far we have been mainly concerned with entities and phenomena occurring within hyperbolic geometry. In Theorem 5, the hyperbolic barycenter $S_{\mathbf{P}}$ of an ideal triangle \mathbf{P} is uniquely

defined by the property that it minimizes the sum of hyperbolic sines of hyperbolic distances to the sides. Now the classical Theorem 1 states that this same S_P happens to coincide with the *least-squares point* L_P , uniquely defined by the property that it minimizes the sum of squares of Euclidean distances to the sides. This strange and unexpected coincidence begs the natural question, for which other ideal polygons it might happen that $S_P = L_P$.

An inscribed Euclidean (resp., ideal hyperbolic) polygon P is *harmonic* if it is obtained from a regular polygon by a projective transformation (resp., hyperbolic isometry) preserving O and its interior. These Euclidean and hyperbolic notions define “the same” inscribed/ideal polygons. Harmonic polygons have been extensively studied since the late 1800s – see for example [6, 17, 20], and the recent [10].

In this section we keep considering “the same” convex P intermittently as an ideal hyperbolic polygon and as an inscribed Euclidean polygon. To avoid cumbersome notation, we keep using the same symbol P , making it clear from context or explicitly each time within which geometry we are working.

As mentioned in the introduction, one of our initial motivations for this work was to find an explanation for the classical but strange Theorem 1. Our main goal in this section is to provide a simple proof of Theorem 33: for every harmonic polygon P , the hyperbolic barycenter S_P and the least-squares point L_P coincide. From this we propose the provocative explanation: $S_P = L_P$ for all triangles P only because all triangles are harmonic.

Denoting by $|X| = \sqrt{x_1^2 + x_2^2}$ the Euclidean norm of a point $X = (x_1, x_2)$, and by $d_t(X)$ the Euclidean distance from X to the line ξ_t , we compute that

$$d_t(X) = \frac{1}{|\xi_t^*|} (1 \mp \xi_t^* \cdot X), \tag{6.1}$$

where the sign depends on whether X and ξ_t^* are on opposite sides or on the same side of ξ_t , respectively. For X in the interior of P , we then compute the gradient

$$\nabla \left(\sum_t d_t^2(X) \right) = 2 \sum_t \left(\frac{\xi_t^* \cdot X - 1}{|\xi_t^*|^2} \right) \xi_t^*. \tag{6.2}$$

From now on we denote by σ_t the Euclidean length of ξ_t .

For the following basic result we include an (unnecessary, but short) argument in the spirit of some of our other computations, to ensure non-circularity.

Lemma 31. *The locus of points X satisfying the Euclidean proportionality condition*

$$[d_{t-1}(X) : \sigma_{t-1}] = [d_t(X) : \sigma_t], \tag{6.3}$$

and contained in the interior of the sector $\angle P_{t-1}P_tP_{t+1}$, is the hyperbolic altitude from P_t to its short diagonal $P_{t-1}P_{t+1}$.

Proof. This is an elementary fact about any triangle $P_1P_2P_3$. Under the parametrization of Section 2, each $|\xi_t^*| = \sec\left(\frac{\varphi_t - \varphi_{t+1}}{2}\right)$ and $\sigma_t = 2 \sin\left(\frac{|\varphi_t - \varphi_{t+1}|}{2}\right)$. The relation $d_1(X)\sigma_2 = d_2(X)\sigma_1$ restricted to our sector defines a line by (6.1) (using the minus signs). Obviously, P_2 is on this line. That ξ_3^* is also on this line is reduced by (6.1) and (2.5) (see also Remark 12) to the short computation that

$$(I_1 + K_1)(I_3 + K_3) - (I_1 - K_1)(I_3 - K_3) - 4J_1J_3 = 1 = (I_2 + K_2)(I_3 + K_3) - (I_2 - K_2)(I_3 - K_3) - 4J_2J_3. \quad \square$$

Theorem 32. *A polygon P is harmonic if and only the hyperbolic altitudes from the vertices to their short diagonals are all concurrent. In this case, the point of concurrence is S_P .*

Proof. One direction is obvious: if P is harmonic then all the hyperbolic altitudes from its vertices to their short diagonals are concurrent at S_P , since these entities are all preserved by any hyperbolic isometry.

To prove the opposite implication, suppose the hyperbolic altitudes from the vertices to the short diagonals of the n -gon \mathbf{P} are concurrent at some S . After a hyperbolic isometry we can assume without loss of generality that $S = (0, 0)$ and $P_t = (\cos(\frac{2\pi t}{n}), \sin(\frac{2\pi t}{n}))$ for $t = 1, 2$. The remaining vertices are now recursively determined: having already fixed P_{t-1} and P_t , the short diagonal $P_{t-1}P_{t+1}$ is uniquely determined by its polar, which lies on the tangent line to \mathbf{O} at P_{t-1} and on SP_t . The vertices of the regular n -gon satisfy the same recurrence and initial conditions, so \mathbf{P} is harmonic. \square

Our Euclidean definition of harmonicity, taken from [20, Section 4], is not the same as the one given in [6, Section VI] and [17, Section 1], which asks for the existence of a point whose distances to the sides are proportional to the side lengths, called the symmedian of \mathbf{P} in [6, Section VI]. Mediated by Lemma 31, Theorem 32 essentially states, from a hyperbolic barycentric perspective, that the two definitions of harmonicity agree. This is not a new result. The first implication in the above proof is essentially already contained in [20, Theorem 4]. A different proof of the opposite implication is given in [17, Section 27] and attributed to Neuberg. Of course, these earlier results simply state that one of the definitions of harmonicity implies the other, and do not refer to hyperbolic altitudes at all. Theorem 32 allows us to eponymously interpret all symmedians as hyperbolic barycenters. The former are defined only for harmonic polygons, whereas the latter are defined in (3.3) for all (convex) ideal hyperbolic polygons.

Theorem 33. *If \mathbf{P} is harmonic then $S_{\mathbf{P}} = L_{\mathbf{P}}$.*

Proof. Let $\sigma := (\sigma_1, \dots, \sigma_n)$ denote the vector of Euclidean side-lengths of \mathbf{P} . For any X , let $\mathbf{d}(X) := (d_1(X), \dots, d_n(X))$ denote the vector of Euclidean distances from X to the sides of \mathbf{P} . Then $\mathbf{d}(X) \cdot \sigma = 2A$, twice the Euclidean area of \mathbf{P} , provided that X is in the interior of \mathbf{P} . Now let $\sigma^\perp(X) := \mathbf{d}(X) - \frac{2A}{|\sigma|^2} \sigma$ denote the orthogonal projection of $\mathbf{d}(X)$ onto the orthogonal complement of $\mathbb{R}\sigma$. Then $|\mathbf{d}(X)|^2 = 4A^2|\sigma|^{-2} + |\sigma^\perp(X)|^2$. Therefore $L_{\mathbf{P}}$, which is by definition the minimizer of $|\mathbf{d}(X)|^2$, is also the minimizer of $|\sigma^\perp(X)|^2$.

In case \mathbf{P} is harmonic, Theorem 32 and Lemma 31 together imply that $\frac{d_{t-1}(S_{\mathbf{P}})}{\sigma_{t-1}} = \frac{d_t(S_{\mathbf{P}})}{\sigma_t}$ for each t . Therefore $\mathbf{d}(S_{\mathbf{P}})$ is a scalar multiple of σ , whence $|\sigma^\perp(S_{\mathbf{P}})|^2 = 0$ and $S_{\mathbf{P}} = L_{\mathbf{P}}$. \square

Remark 34. The coordinates of the symmedian S of a triangle have been obtained explicitly in [5], in terms of the equations of the lines formed by the sides of the triangle, using the optimality property in Theorem 1 as a defining property of S . In principle, the coordinatization of [5] and ours in (3.3) could be deduced directly from one another by a series of presumably unenlightening algebraic manipulations. Theorem 33, which contains Theorem 1 as its first special case, can be understood as a more conceptual explanation for the agreement of the two coordinatizations.

We see from the proof of Theorem 33 that $L_{\mathbf{P}}$ is equivalently characterized as the minimizer of $|\sigma^\perp(X)|$, which achieves 0 as its minimum value precisely when \mathbf{P} is harmonic, by Theorem 32. In principle, one can express $L_{\mathbf{P}}$ algebraically in terms of p_1, \dots, p_n by setting the right-hand side of (6.2) to zero. The condition $S_{\mathbf{P}} = L_{\mathbf{P}}$ defines a subspace of codimension at most 2 in the space \mathcal{P}_n of all ideal n -gons (cf. Section 5). On the other hand, the subspace of \mathcal{P}_n consisting of harmonic n -gons is three-dimensional, and therefore the space of n -gons for which $S_{\mathbf{P}} = L_{\mathbf{P}}$ must strictly contain the space of harmonic n -gons for $n > 5$. This can maybe be understood as some kind of “regularity condition” on \mathbf{P} , which is in general strictly weaker than harmonicity. And yet, according to the following result, harmonicity is (nearly) equivalent to having $S_{\mathbf{P}} = L_{\mathbf{P}}$ in the next case $n = 4$.

Theorem 35. *If \mathbf{P} is a quadrilateral, then $S_{\mathbf{P}} = L_{\mathbf{P}}$ if and only if either \mathbf{P} is harmonic or else $S_{\mathbf{P}} = (0, 0)$.*

Proof.

(\Leftarrow). It follows from Theorem 18 that $S_{\mathbf{P}} = (0,0)$ if and only if the Euclidean polygon \mathbf{P} is a rectangle, in which case it is clear that $L_{\mathbf{P}} = (0,0)$. If \mathbf{P} is harmonic then $S_{\mathbf{P}} = L_{\mathbf{P}}$ by Theorem 33.

(\Rightarrow). Setting to zero the evaluation of (6.2) at $X = S_{\mathbf{P}}$, after some algebraic manipulation, we conclude that either $I_{\mathbf{P}} - K_{\mathbf{P}} = 0 = J_{\mathbf{P}}$, or else the cross-ratio $[p_1, p_2, p_3, p_4] = 1$. These conditions are equivalent to having $S_{\mathbf{P}} = (0,0)$ and to \mathbf{P} being harmonic, respectively. \square

The conclusion of Theorem 35 may seem strange, because the origin is only special from the Euclidean point of view, but hyperbolically unremarkable. But the origin remains meaningful when comparing the two geometries, since the endofunctions of the unit disc which are simultaneously hyperbolic and Euclidean isometries are precisely the rotations about the origin.

7. Remaining questions

In this section we gather some questions concerning hyperbolic barycenters, which arose during the preparation of this manuscript and for which we do not yet have definitive answers and which we believe deserve further study.

7.1. The role of convexity

The minimality result in Theorem 5 holds only for *convex* ideal hyperbolic polygons. In the case of non-convex ideal hyperbolic polygons, what happens is that $\mathcal{Q}(\mathbf{x}) := \sum_t \sinh(d(\mathbf{x}, \xi_t))$ and $\mathcal{L}_+(\mathbf{x}) := |\langle \mathbf{x}, \sum_t \xi_t^* \rangle|$ only agree on the region of \mathbb{H} consisting of points \mathbf{x} that are all on the same side of each ξ_t relative to each principal polar ξ_t^* . For convex polygons, we showed that \mathcal{Q} could only be minimized in the interior of \mathbf{P} , where \mathcal{Q} and \mathcal{L}_+ do agree, and in this case we were even able to show as a consequence of Corollary 14 that $S_{\mathbf{P}}$ lies in the interior of \mathbf{P} , whence a posteriori the vector $\sum_t \xi_t^*$ lies in the interior of the light cone \mathbb{L} .

None of this is guaranteed in the non-convex case. For each *signature* $\beta: \{1, \dots, n\} \rightarrow \{+, -\}$, let us consider the corresponding (possibly empty) region $\mathbb{H}_\beta := \{\mathbf{x} \in \mathbb{H} \mid \langle \mathbf{x}, \xi_t^* \rangle \in \mathbb{R}_{\beta(t)}\}$, where \mathbb{R}_+ (resp., \mathbb{R}_-) denotes the non-negative (resp., non-positive) real numbers. Then $\mathcal{Q}(\mathbf{x})$ restricted to \mathbb{H}_β agrees precisely with $\mathcal{L}_\beta(\mathbf{x}) := |\langle \mathbf{x}, \sum_t \beta(t) \xi_t^* \rangle|$. But we cannot conclude that the minimizer of \mathbb{H} of the latter function is a scalar multiple of $\sum_t \beta(t) \xi_t^*$, because we do not even know in general why this vector should be in the interior of the light cone, and even if it is, it is not obvious that its normalization belongs to the correct region \mathbb{H}_β .

Another intriguing and complementary possibility would be to replace the hyperbolic distances $d(\mathbf{x}, \xi_t)$ occurring in $\mathcal{Q}(\mathbf{x})$ with the *signed* distances $\frac{\langle \mathbf{x}, \xi_t^* \rangle}{|\langle \mathbf{x}, \xi_t^* \rangle|} d(\mathbf{x}, \xi_t)$, which would have the practical effect of essentially replacing $\mathcal{Q}(\mathbf{x})$ with $\mathcal{L}_+(\mathbf{x})$ as the function to be optimized, and yield the normalization of $\sum_t \xi_t^*$ as a critical point. Or, as we already mentioned in Remark 8, one could instead follow [4] in defining the hyperbolic barycenter dynamically as the fixed point of the composition of the infinitesimal rotations along the sides of \mathbf{P} . One can show that the axis is still spanned by $\sum_t \xi_t^*$, but there is again no guarantee that this vector is timelike. So, it is a priori possible that the “hyperbolic barycenter” of a non-convex ideal polygon may be outside of \mathbb{H} , possibly in de Sitter space \mathcal{S} , or even possibly somewhere on the light cone \mathbb{L} .

7.2. Comparison with other polygonal centers

Let us briefly compare the hyperbolic barycenter $S_{\mathbf{P}}$ with other centers defined by integrable polygonal dynamics, optimality conditions, and least-action principles.

As we already mentioned in Section 3, the cross-ratio dynamics of [4] form a kind of ideal hyperbolic analogue of the bicycle correspondence of [18], making the hyperbolic barycenter of an ideal hyperbolic polygon analogous to the circumcenter of mass of a Euclidean polygon. When we consider an ideal hyperbolic polygon (in the Beltrami–Cayley–Klein model) as a Euclidean polygon, it is evidently inscribed in the absolute, whence its circumcenter of mass trivially coincides with the origin. Thus the hyperbolic barycenter can be considered also as a meaningful analogue of the circumcenter of mass, for an inscribed Euclidean polygon. Indeed, it would be interesting to characterise the circumcenter of mass, analogously with our Theorem 5, by means of some least-action principle, i.e., as a kind of barycenter. One promising such characterisation might come from the fact that the circumcenter of the triangle is the point minimizing the area of its contact triangle (i.e. the triangle formed by the feet of the perpendiculars from the point to the sides).

As discussed in Section 6, the hyperbolic barycenter $S_{\mathbf{P}}$ of a harmonic ideal hyperbolic n -gon agrees with the least-squares point $L_{\mathbf{P}}$ of the corresponding Euclidean polygon. Thus asking for these points to agree can be understood as a kind of weakening of harmonicity, as we saw in Theorem 35. We expect that a similar algebraic analysis should yield the following case $n = 5$. One subtlety in this case is that the regular pentagram \mathbf{P} still satisfies the proportionality condition $\sigma^{\perp}(S_{\mathbf{P}}) = \mathbf{0}$, and therefore so do all of its images under hyperbolic isometry. Although this \mathbf{P} is not “harmonic” in our sense, the subspace of \mathcal{P}_5 defined by $S_{\mathbf{P}} = L_{\mathbf{P}}$ does not consist only of convex polygons. Allowing for this subtlety, we still optimistically hope for the best possible result.

Conjecture 36. *If $\mathbf{P} = (p_1, \dots, p_5)$ is a pentagon, then $S_{\mathbf{P}} = L_{\mathbf{P}}$ if and only if either the five cross-ratios $[p_t, p_{t+1}, p_{t+2}, p_{t+3}]$ are all the same or $S_{\mathbf{P}} = (0, 0)$.*

Yet another infamous polygonal center is the fixed point of the pentagram map, which was discovered in [16] and coordinatized in [11]. In [1, Section 1] it is suggested that this point may be the limit point as $\varepsilon \rightarrow 0$ of an eigenvector for the infinitesimal monodromy of a deformation into twisted polygons $\mathbf{P}_{1+\varepsilon}$ of a closed polygon \mathbf{P}_1 (cf. Remark 8). And yet, it remains unknown whether the circumcenter of mass or the fixed point of the pentagram map is defined by an optimality property analogous to that of the hyperbolic barycenter in Theorem 5. We refer to [13] for a systematic discussion of polygonal centers defined by optimality conditions and least-action principles.

7.3. Moduli spaces

In Section 5 we were able to find interesting algebro-geometric descriptions of the moduli spaces $\mathcal{M}_n(S)$ of ideal hyperbolic n -gons with fixed barycenter $S \in \mathbb{H}$ for the smallest values of $n = 3, 4$. It is tempting to try to continue this story for higher values of n .

The five polars of an ideal pentagon \mathbf{P} define a unique conic Γ , which again by the Poncelet porism yields a one-parameter family of pentagons circumscribed in (Γ, \mathbf{O}) . Though it might seem natural to hope for all these pentagons to share the same hyperbolic barycenter $S_{\mathbf{P}}$, we have verified experimentally that they do not. We leave open the tantalizing question of how to parameterize, in a similarly algebro-geometric manner as we have done for triangles in Theorem 26 and for quadrilaterals in Theorem 28, the corresponding moduli spaces for ideal hyperbolic n -gons for $n \geq 5$, beyond the obvious algebraic conditions (5.1).

Acknowledgements

Both authors are thankful to Serge Tabachnikov, Ivan Izestiev, and the anonymous referee for their insightful comments and valuable suggestions.

Declaration of interests

The authors do not work for, advise, own shares in, or receive funds from any organization that could benefit from this article, and have declared no affiliations other than their research organizations.

References

- [1] Q. Aboud and A. Izosimov, “The limit point of the pentagram map and infinitesimal monodromy”, *Int. Math. Res. Not.* **2022** (2022), no. 7, pp. 5383–5397.
- [2] A. V. Akopyan, “On some classical constructions extended to hyperbolic geometry”, *Mat. Prosvesh.* **3** (2009), no. 13, pp. 155–170.
- [3] A. V. Akopyan, *Geometry in figures*, CreateSpace Independent Publishing Platform, 2017.
- [4] M. Arnold, D. Fuchs, I. Izmetiev and S. Tabachnikov, “Cross-ratio dynamics on ideal polygons”, *Int. Math. Res. Not.* **2022** (2022), no. 9, pp. 6770–6853.
- [5] M. Bani-Yaghoub, N. H. Rhee and J. Sadek, “An algebraic method to find the symmedian point of a triangle”, *Math. Mag.* **89** (2016), no. 3, pp. 197–200.
- [6] J. Casey, “Supplementary chapter”, in *A Sequel to the First Six Books of the Elements of Euclid*, 5th edition, Hodges, Figgis, & Co., 1888, pp. 165–222.
- [7] H. S. M. Coxeter, *The real projective plane*, Third edition, Springer, 1993, pp. xiv+222.
- [8] K. Drach and R. E. Schwartz, “A hyperbolic view of the seven circles theorem”, *Math. Intell.* **42** (2020), no. 2, pp. 61–65.
- [9] V. Dragović and M. Radnović, *Poncelet porisms and beyond. Integrable billiards, hyperelliptic Jacobians and pencils of quadrics*, Birkhäuser/Springer, 2011, pp. viii+293.
- [10] R. A. Garcia, D. Reznik and P. Roitman, “New properties of harmonic polygons”, *J. Geom. Graph.* **26** (2022), no. 2, pp. 217–236.
- [11] M. Glick, “The limit point of the pentagram map”, *Int. Math. Res. Not.* **2020** (2020), no. 9, pp. 2818–2831.
- [12] R. Honsberger, *Episodes in nineteenth and twentieth century Euclidean geometry*, Mathematical Association of America, 1995, pp. xiv+174.
- [13] M. J. Kaiser and T. L. Morin, “Characterizing centers of convex bodies via optimization”, *J. Math. Anal. Appl.* **184** (1994), no. 3, pp. 533–559.
- [14] J. S. Mackay, “Early History of the Symmedian Point”, *Proc. Edinb. Math. Soc.* **11** (1892), pp. 92–103.
- [15] W. F. Reynolds, “Hyperbolic geometry on a hyperboloid”, *Am. Math. Mon.* **100** (1993), no. 5, pp. 442–455.
- [16] R. E. Schwartz, “The pentagram map”, *Exp. Math.* **1** (1992), no. 1, pp. 71–81.
- [17] T. C. Simmons, “A new Method for the Investigation of Harmonic Polygons”, *Proc. Lond. Math. Soc.* **18** (1886), pp. 289–304.
- [18] S. Tabachnikov and E. Tsukerman, “On the discrete bicycle transformation”, *Publ. Mat. Urug.* **14** (2013), pp. 201–219.
- [19] S. Tabachnikov and E. Tsukerman, “Circumcenter of mass and generalized Euler line”, *Discrete Comput. Geom.* **51** (2014), no. 4, pp. 815–836.
- [20] G. Tarry and J. Neuberg, “Sur les polygones et les polyèdres harmoniques”, in *Association Française pour l’Avancement des Sciences, Compte Rendu de la 15e Session - Nancy 1886(Seconde Partie – Notes et Mémoires)*, 1887, pp. 12–24.